IOD: THE ROMANIAN ACADEMY
ICA: INSTITUTE OF CHEMISTRY TIMISOARA OF ROMANIAN ACADEMY

BOGDAN-OVIDIU ȚĂRANU

CONTRIBUTIONS TO THE PHYSICAL-CHEMICAL CHARACTERIZATION OF PORPHYRINS. SENSOR AND CORROSION APPLICATIONS

Ph.D. THESIS ABSTRACT

Ph.D. COORDINATOR

Senior Researcher Ph.D. Eng. EUGENIA FĂGĂDAR-COSMA

2016

TABLE OF CONTENTS

Keywords: porphyrins; metalloporphyrins; TEM microscopy; corrosion; potentiometric sensors; SEM microscopy; AFM microscopy; cyclic voltammetry; corrosion inhibition.

INTRODUCTION

The present Ph.D. thesis - that is positioned at the interface between Fundamental and Applied Chemistry - is focused on the study of porphyrins and addresses a border area between different disciplines of chemistry, such as: - microscopy, electrochemistry, analytical chemistry and corrosion. Porphyrins are a class of biomimetic macrocyclic compounds exhibiting extended aromatic character, outstanding optoelectronic properties and are suitable for the development of Sustainable Chemistry.

The interdisciplinary nature of the thesis is given by the need for systematic and exhaustive characterization of novel porphyrin and metalloporphyrin structures and by the identification of potential applications. The study of the self-assembly and self-organization ability of porphyrins by varying the solvent type, the substrate type, even the surface confinement and the liquid/gas interface, using advanced microscopy techniques proved essential for establishing some aggregation mechanisms. The information obtained from characterization studies included fundamental scientific information that helps improve the knowledge in the very promising field of porphyrin chemistry, as well as information that helps to identify some useful applications of the porphyrin derivatives. Thus, possible applications for porphyrins were identified in sensors formulation and the corrosion protection of steel, two areas of great interest for analytical chemistry, early medical diagnosis, environmental protection and industry.

Symmetrically *meso*-substituted A_4 or mixed asymmetrically substituted A_3B porphyrins synthesized in IOD laboratory, some with novel structures or that have never been analysed in these specific conditions by using modern equipment that allowed their detailed investigation, were used throughout the studies described in the Ph.D. thesis. The systematic characterization of porphyrin derivatives, including their electrochemical and aggregation behavior, was performed using physical-chemical methods, such as: cyclic voltammetry, transmission and scanning electron microscopy, atomic force microscopy, electron tomography and X-ray diffraction. Furthermore, corrosion studies were performed with the purpose of discovering new corrosion inhibitors having macrocyclic tetrapyrrole structure. Novel efficient potentiometric sensors for cation and anion detection were formulated and are based on the novel porphyrin structures.

The main objective of the Ph.D. thesis is to provide novel and outstanding contributions to the fundamental chemistry of porphyrins by expanding the current database through the physical-chemical analysis of some free base and metallated porphyrins, using advanced and scientifically accurate analytical methods, as well as to identify noteworthy applications in sensors and the corrosion inhibition of steel in aggressive acidic media.

The structure of the thesis consists of six chapters, as follows:

Chapter 1 presents an extensive literature study focused on theoretical aspects concerning porphyrins and porphyrin-based hybrid materials regarding their ability to generate porphyrin

aggregates, up-to-date information acquired using cyclic voltammetry and on basic notions about the use of porphyrins in the manufacturing of ion-selective potentiometric sensors.

Chapter 2 describes the advanced equipment used during the scientific experiments.

Chapter 3 presents the investigation of the aggregation behavior of some free base and metallated porphyrins using various physical-chemical methods, as well as studies performed on porphyrin-based hybrid materials. The originality of the results is given by the information acquired from porphyrin and hybrid material characterizations - that have never been studied in such detail and also by the progress made in clarifying some aggregation mechanisms.

Chapter 4 continues the study of the porphyrin derivatives, but this time in terms of their electrochemical behavior, using cyclic voltammetry. The experimental results clearly show the ability of the porphyrin macrocycle to undergo both oxidation and reduction processes, irrespective of substituents nature and working electrode type, of the presence or absence of the central metal ion and of electrolysis conditions.

Chapter 5 is dedicated to the manufacturing of novel ion-selective electrodes using porphyrins as ionophores, all sensors described in this chapter representing an original contribution of the Ph.D. thesis.

Chapter 6 deals with the actual issue of corrosion protection by investigating the corrosion inhibition properties of a free base porphyrin in the case of carbon steel corrosion in aggressive acidic media.

EXPERIMENTAL RESULTS AND DISCUSSION

Characterization of some porphyrins and porphyrin-based hybrid materials using microscopy techniques.

The ability of porphyrins and porphyrin-based hybrid materials to self-assemble and self-organize was investigated using physical-chemical methods, especially microscopy techniques, in order to acquire morphological and topographical information about the observed aggregates. Images recorded during porphyrin sample analyses highlighted the versatile nature of these compounds that formed a wide variety of aggregates. Among the many observed porphyrin architectures there were: toroidal and leaf-like aggregates, rods, irregular polygons, circular and quasi-circular islands, spheres, bundles, dendritic, worm-like and butterfly-shaped aggregates.

The self-aggregation and self-organization of porphyrin molecules into different structures is influenced by many parameters, including: the solvent type, the nature of the substrate, the confinement of the substrate surface, the number of deposited layers etc.

The studies allowed the identification of “pinhole” and “coffee stain” mechanisms, partially responsible for the generated architectures, while electron tomography highlighted - for the first time - the compact internal architecture of some porphyrin aggregates.

Remarkable results were obtained when 5,10,15,20-tetra(*p*-tolyl)porphyrin was applied from tetrahydrofuran solution on TEM grids. The porphyrin formed toroidal and leaf-like structures that coexisted under different association stages (Fig. 1). Such biomorphic formations, similar to water lilies or centred ferns have not been previously reported in the literature - in the context of porphyrin aggregates.

The rod-like structures observed on the 5,10,15,20-tetrakis(4-allyloxyphenyl)porphyrin samples obtained under the same conditions are also noteworthy. The length of the rods was in the micrometre range, meaning that they are longer than the ones reported in the literature for this type of porphyrin aggregates.

The ring structures formed by the same porphyrin when deposited on TEM grids from dichloromethane solution can be explained by the "pinhole" mechanism [1], considering that this solvent is well capable of wetting the hydrophobic surface of the carbon coated grid. It is important to mention that the helical aggregation of porphyrins through successive J and H type processes significantly contributed to the formation of the ring structures [2].

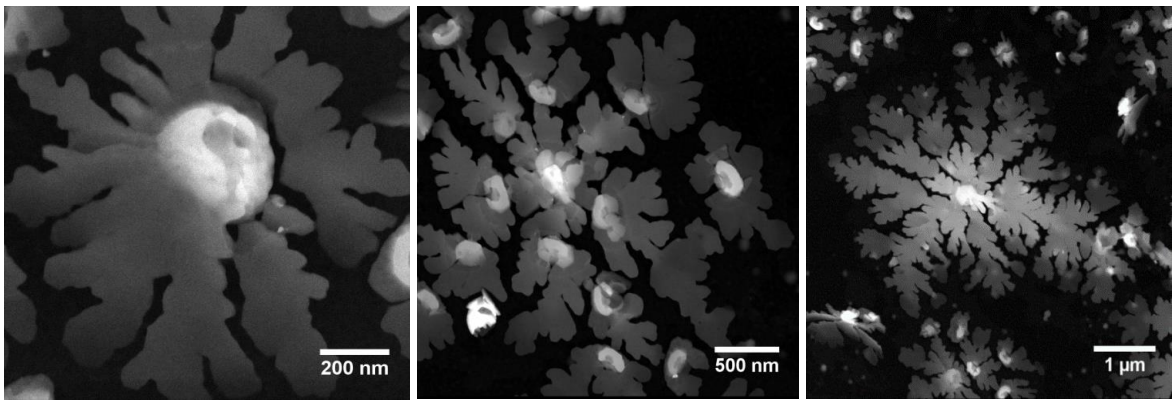

Fig. 1. STEM images recorded for the 5,10,15,20-tetra(*p*-tolyl)porphyrin sample.

The information obtained from TEM and STEM analysis of the porphyrins aggregation behavior was complemented by SEM and AFM analyses that also revealed numerous types of morphologies, such as: ovoidal grains and islands, qvasi-hexagonal tablets, rods, branched and unbranched needles, dendritic, worm-like and fractal border shaped aggregates.

The dependence between the morphology of porphyrin aggregates and the number of deposited porphyrin layers was evidenced in the case of 5,10,15,20-tetra(*p*-tolyl)porphyrin with noteworthy results. Deposition of the first porphyrin layer favored J-type aggregation processes and as a result, fractal structures were formed. Increasing the number of porphyrin layers resulted in the considerable involvement of H-type aggregation processes and new aggregates were observed, including quasi-hexagonal tablets.

The presence of a channel along the middle of the leaf-like structures, as evidenced by AFM analysis, indicated their growth via a clockwise and counter clockwise helical process [2].

The macroscopic ring observed on Zn(II) 5,10,15,20-tetra(4-*N*-methylpyridinium) porphyrin tetrachloride samples, deposited from aqueous solution on glassy carbon pellets, can be

explained by the "coffee stain" mechanism [1], considering that the polarity of water and the hydrophobicity of the glassy carbon prevented the proper wetting of this surface by the solution droplet.

X-ray diffraction analysis showed that for some structures, the dissolution of porphyrins in different solvents and their subsequent deposition on a monocrystalline silicon substrate leads to different crystalline forms than the ones observed for porphyrin powder samples. This difference can be explained by the ability of porphyrins to absorb large amounts of gases from the atmosphere and also to form clathrates by intercalating solvent molecules between porphyrin host layers [3].

The aggregation behavior of porphyrin-based plasmonic (with gold nanoparticles) and polymeric (polyvinylpyrrolidone) hybrid materials was also studied using microscopy techniques.

The experiments focused on the interaction between metalloporphyrins and colloidal gold and showed that the presence of colloidal gold had no significant effect on the morphology of the porphyrin aggregates formed by the self-assembly of water-soluble Zn(II) 5,10,15,20-tetra (4-*N*-methylpyridinium)porphyrin tetrachloride, while the interaction between the gold nanoparticles and Co(II) 5,10,15,20-tetrakis(3-hydroxyphenyl)porphyrin, deposited from tetrahydrofuran, resulted in the formation of discoidal and dendritic aggregates (Fig. 4) - that formed surfaces exhibiting remarkable electocatalitic properties for the detection of trace quantities of H_2O_2 [4].

The microscopic characterization of the polyvinylpyrrolidone - 5-(4-pyridyl)-10,15,20-tris (phenoxyphenyl)porphyrin hybrid material was part of a larger study, aimed at investigating the behavior of the material in solutions for applications regarding the CO_2 detection [5]. The samples obtained from aqueous solutions containing the hybrid material were prepared with and without CO_2 bubbling. Gas exposure changed the morphology of the observed structures because of CO_2 absorption by the hybrid material. This absorption mechanism was proved by AFM analysis.

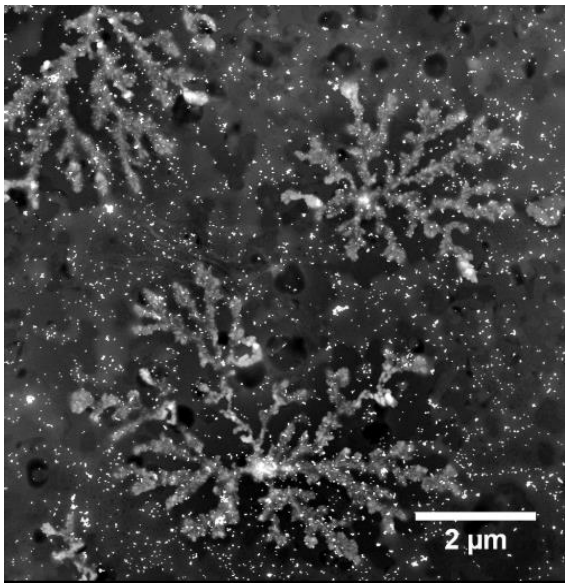

Fig. 4. Dendritic aggregates observed on samples resulted from the interaction between colloidal gold and Co(II) 5,10,15,20-tetrakis(3-hydroxyphenyl)porphyrin.

Characterization of some porphyrin and metalloporphyrin derivatives using cyclic voltammetry.

The electrochemical properties of porphyrins were highlighted using cyclic voltammetry in order to identify the occurring electrode processes and the influence of electronic effects brought by the substituents on the potential values. The oxidation and reduction processes occurring at the porphyrin macrocycle were identified for all studied porphyrins and the mono- and dicationic species generated during the cyclic voltammetry experiments were supplementary evidenced using UV-Vis spectroscopy.

The electrochemical behavior of free base porphyrins was studied on the Pt and glassy carbon electrodes using benzonitrile or dichloromethane as solvent and tetrabutylammonium perchlorate as the supporting electrolyte. During the cyclic voltammetry experiments (Fig. 5), the porphyrin derivatives were oxidized in two stages at the extended π-aromatic system, resulting in the formation of π-cation radicals and dications. The differences between the potentials of the two anodic signals from one porphyrin structure to another were attributed to the competition between several effects brought by the substituents nature, namely: electronic, steric and extended conjugation effects involving the macrocycle. Thus, the methyl substituents of 5,10,15,20-tetra (*p*-tolyl)porphyrin have a weak electron-donating inductive effect; in case of 5-(4-pyridyl)-10,15,20-tris(phenoxyphenyl)porphyrin the extended aromatic conjugation is interrupted by the distortion of the macrocycle planarity and this is accompanied by the steric effects due to the phenoxy-phenyl groups. In case of 5,10,15,20-tetrakis(4-allyloxyphenyl)porphyrin, the double bonds of the *meso*-phenyl substituents extend the conjugation with the porphyrin macrocycle favouring the oxidation processes.

The short-life species generated during the electrochemical characterization of free base porphyrins in electrolyte solutions containing dichloromethane was evidenced by comparing the UV-Vis spectra acquired during the electrochemical experiments with those obtained in fresh solutions (Fig. 5). The protonation of the inner nitrogen atoms of the porphyrin macrocycle was responsible for the splitting of the Soret band. One of the two new bands was located at the same wavelength as the Soret band of the unmodified porphyrin, while the other was significantly bathochromically shifted. A bathochromic shift was also observed for the QI band accompanied by a hyperchromic effect. These modifications indicate the formation of mono- and diprotonated intermediate species [2].

In the case of metalloporphyrins, the cyclic voltammetry characterization of Co(II) 5,10,15,20-tetrakis(3-hydroxyphenyl)porphyrin at the Pt electrode highlighted processes occurring at the porphyrin macrocycle and also due to the central metal ion. Three oxidation and three reduction waves were observed in the anodic potential range (Fig. 6). The first oxidation wave was irreversible and did not form a redox couple with the reduction wave at ~ 0.25 V.

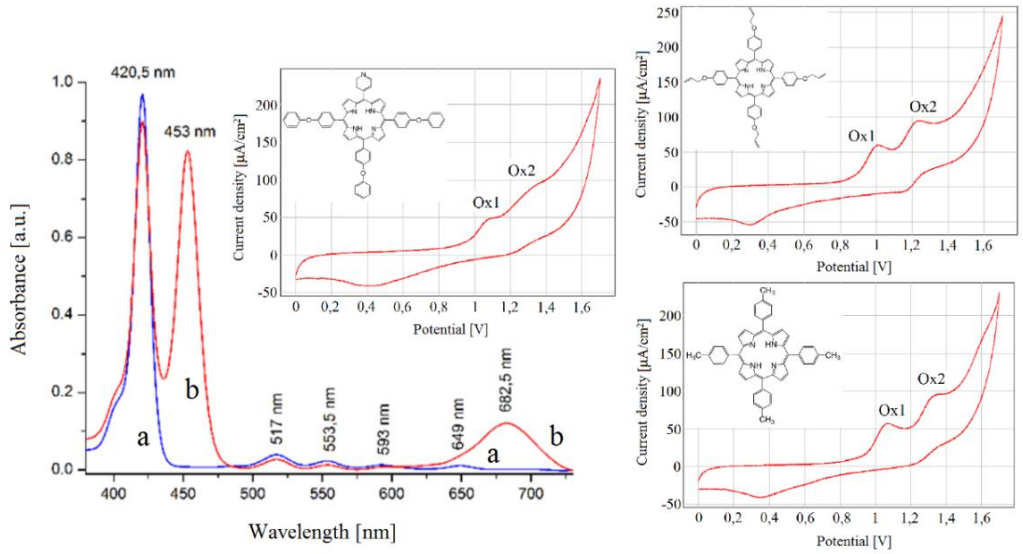

Fig. 5. Cyclic voltammograms recorded in the anodic potential range in porphyrin solutions and UV-Vis spectra recorded before (a) and during the electrochemical experiments (b).

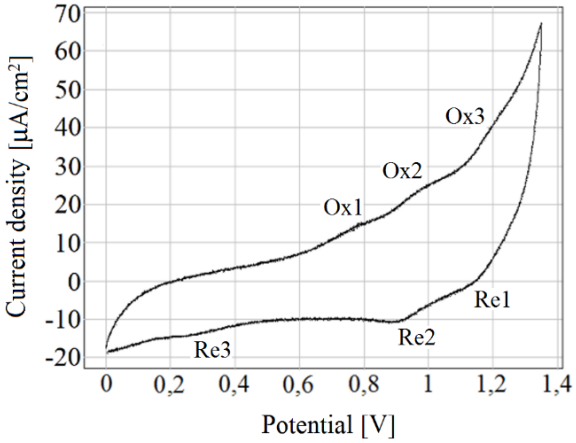

Fig. 6. Cyclic voltammogram recorded in electrolyte solution containing Co(II) 5,10,15,20-tetrakis(3-hydroxyphenyl)porphyrin, in the anodic potential range.

This kind of situation was previously observed during voltammetry studies performed on cobalt porphyrins and the phenomenon was attributed to the involvement of an axial ligand in the oxidation reaction [6].

Reactions (1), (2) and (3) were attributed to the three oxidation waves by taking into account the previously mentioned study, as well as other studies reported in the literature [7]. The first reaction is the oxidation of Co(II) to Co(III) and the other two take place at the porphyrin macrocycle, as illustrated by reaction equations (1-3).

$$Co(II)TOHPP + A^- \rightarrow Co(III)TOHPP(A) + e^- \quad (1)$$

$$Co(III)TOHPP(A) \rightarrow [Co(III)TOHPP(A)]^+ + e^- \quad (2)$$

$$[Co(III)TOHPP(A)]^+ \rightarrow [Co(III)TOHPP(A)]^{2+} + e^- \quad (3)$$

Where A^- = anion present in the solvent - supporting electrolyte system

Another reaction occurring at the central metal ion (4) was attributed to the reduction wave observed in the cathodic potential range, in accordance with the literature [7].

$$Co(II)TOHPP + e^- \rightarrow [Co(I)TOHPP]^- \quad (4)$$

Porphyrin applications in sensors. The manufacturing and evaluation of some potentiometric sensors using porphyrins as ionophores.

Based on the properties of free base and metallated porphyrins to coordinate metal ions and/or axial ligands that make them suitable for use in the development of electrochemical sensors, several novel porphyrin structures were selected as ionophores and were incorporated in the polyvinyl chloride membranes for formulation of some cation- or anion-selective electrodes. The detection properties of the sensors were evaluated using the separate solution method, by preparing cationic and anionic solutions having different concentrations. Different types of plasticizers were used to plasticize the membranes and the importance of plasticizer selection on the detection properties of metalloporphyrin-based sensors was also evidenced.

In one study, 5-(4-pyridyl)-10,15,20-tris(phenoxyphenyl)porphyrin was successfully used to manufacture and evaluate a Cr^{3+} sensor with remarkable selectivity [8]. The detection of Cr^{3+} ions is important both for an early medical diagnosis and for environmental monitoring. The sensor showed a slope of 18.11 mV/decade over the $3 \times 10^{-5} \div 10^{-1}$ M concentration range with a detection limit of 9×10^{-6} M. Based on its pH function the sensor could be used in the acidic pH range from 2 to 5.5.

The ability of metalloporphyrins to selectively detect anions when used as ionophores in ion-selective electrodes was demonstrated by the manufacturing and testing of a perchlorate-selective potentiometric sensor. Perchlorate detection is known as important both for medical and industrial purposes. In order to identify the best metalloporphyrin ionophore, three different A_4 metalloporphyrins: Zn(II) 5,10,15,20-tetra(*p*-tolyl)porphyrin, Zn(II) 5,10,15,20-tetrakis (4-allyloxyphenyl)porphyrin and Co(II) 5,10,15,20-tetrakis(3-hydroxy-phenyl)porphyrin were used to manufacture ion-selective electrodes with membranes plasticized using *o*-nitrophenyl-octylether. All three electrodes showed selectivity toward the perchlorate ion. The best potentiometric response was observed for the sensor using Co(II) 5,10,15,20-tetrakis(3-hydroxy-phenyl)porphyrin as ionophore. An optimization study conducted to improve the sensor properties consisted in obtaining several membranes incorporating the porphyrin, but plasticized with other different plasticizers, namely: dioctylphtalate and dioctylsebacate. The membrane showing the best perchlorate sensor detection was plasticized with dioctylphtalate. The sensor exhibited a near-Nernstian slope of 58.95 mV/decade in the $5 \times 10^{-7} \div 10^{-1}$ M perchlorate concentration range, a detection limit of 3×10^{-7} M and was stable in the pH range 2.5 ÷ 12. These outstanding features placed this sensor among the best perchlorate-selective potentiometric sensors reported in the literature.

A study based on the metalloporphyrin structure Zn(II) 5,10,15,20-tetrakis(3,4-dimethoxy-phenyl)porphyrin demonstrated the importance of plasticizer selection on the selectivity properties of potentiometric sensors. Using this porphyrin as ionophore led to the manufacturing of perchlorate-, thiocyanate- and iodide-selective electrodes. Thus, a sensor with selectivity and sensibility toward the perchlorate ion was manufactured using dioctylphtalate as plasticizer and showed a slope of 59.15 mV/decade in the $10^{-6} \div 10^{-1}$ M concentration range of perchlorate ions. The use of dioctylsebacate as plasticizer resulted in the manufacturing of a thiocyanate-selective sensor with a slope of 59.21 mV/decade in the $10^{-5} \div 10^{-1}$ M concentration range. In terms of selectivity, in this case the perchlorate anion was identified as an interfering ion. Incorporating the same metalloporphyrin ionophore an iodide-selective electrode with *o*-nitrophenyloctylether plasticized membrane was also manufactured and tested. The sensor showed a slope of 56,59 mV/decade in the $10^{-6} \div 10^{-1}$ M concentration range, while the values of the potentiometric selectivity coefficients indicated both perchlorate and thiocyanate as interfering ions.

The influence of 5,10,15,20-tetrakis(4-pyridyl)porphyrin on the corrosion of steel in aqueous sulphuric acid solution. Characterization of samples by AFM technique.

One of the many properties of porphyrins is their ability to act as corrosion inhibitors. Based on this observation, the corrosion inhibition ability of 5,10,15,20-tetrakis(4-pyridyl) porphyrin in case of carbon steel samples in aggressive acidic media (H_2SO_4 5%) was investigated and demonstrated [9]. The corrosive environment provided an accelerated corrosion process with measurable effects over a short time period. The influence of porphyrin concentration and temperature on the corrosion rate on the metal surface was investigated throughout the study. The corrosion rate decreased when the porphyrin was present in the corrosive environment and the dependence of corrosion rate on porphyrin concentration, for the studied temperature ranges, showed the greater influence of the compound at higher temperatures and lower concentrations (Fig. 7A). Above a certain concentration the decrease of the corrosion rate became less pronounced, probably because the porphyrin completely covered the surface of the samples with a film having limited stability in the acidic solution.

AFM surface analysis of samples exposed to the acidic environment in the presence of the porphyrin evidenced its smoothing and levelling effect (Fig. 7B) by comparison with the surface of the samples exposed to the same environment, but without porphyrin.

The images recorded during AFM analysis also showed the presence of porphyrin aggregates made of prism-shaped units having a triangular base, formed as a result of molecular self-assembly through J and H type processes that contributed to the decrease of the corrosion rate by covering the metal surface with compact multilayer structures. Both temperature and concentration affected the inhibiting action of the porphyrin in the corrosive environment and the results showed an inhibition efficiency greater than 50% for the carbon steel samples (table 1).

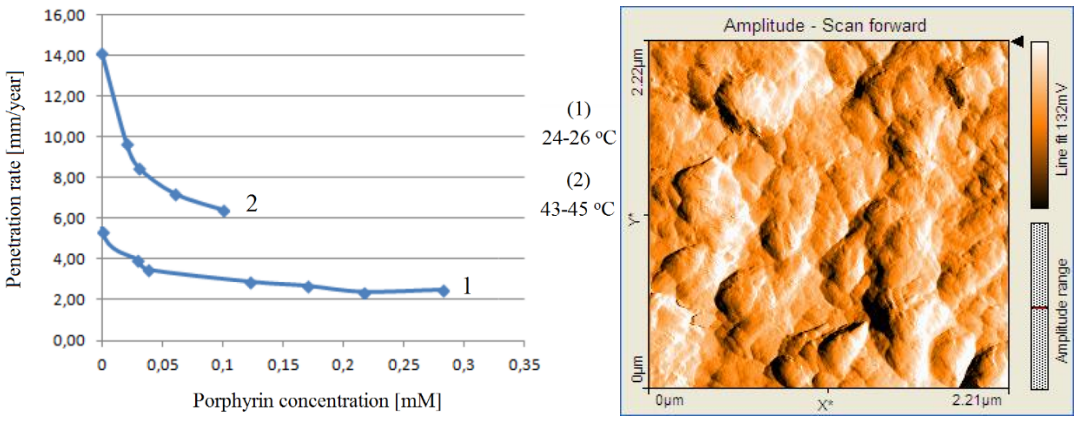

A B

Fig. 7. A) Dependence of corrosion rate on porphyrin concentration for the 24-26 °C temperature range (1) and for the 43-45 °C temperature range (2). B) AFM image recorded on the surface of a carbon steel sample corroded in H_2SO_4 5% solution containing the porphyrin.

Table 1. AFM topography results obtained for the surfaces of carbon steel samples corroded in the acidic solution with and without porphyrin, in the temperature ranges that produced the best inhibition effect

c_{porf} *[mM]*	t^o *[°C]*	*Surface roughness [nm]*	*Maximum peak height [nm]*	*Maximum valley depth [nm]*	*Corrosion inhibition efficiency [%]*
0,23	25-26	21	68	-110	55,5
Without porphyrin	25-26	36	130	-130	-
0,10	42-43	32	120	-150	54,3
Without porphyrin	42-43	46	150	-180	-

GENERAL CONCLUSIONS

- The experimental results and the original contributions of the Ph.D. thesis proved that its objectives concerning the expansion of the current knowledge by physical-chemical characterization of some *meso*-substituted porphyrins and metalloporphyrins, using various advanced and scientifically accurate analytical methods and the identification of noteworthy applications in the manufacturing of new sensors and the corrosion inhibition of steel in acidic media were fulfilled.
- The study by various physical-chemical methods, especially advanced microscopy techniques regarding the aggregation behavior of some porphyrins and porphyrin-based hybrid materials that have not been investigated under the specified conditions and in such depth, resulted in the acquisition of original data and clarification of some aggregation mechanisms.

- The versatile nature of the studied porphyrins was responsible for the formation of a wide variety of morphologically distinct aggregates, including novel bimorph structures that have not been previously reported in the literature.
- The use of electron tomography to investigate the porphyrin aggregates constitutes a novelty element and it showed for the first time the compact internal architecture of these structures.
- X-ray diffraction data revealed that depending on the solvent type, porphyrin molecules can undergo recrystallization phenomena resulting in novel crystalline forms. The process is due to the capacity of porphyrins to absorb large amounts of gases from the atmosphere and/or solvent molecules to form clathrates.
- The studies conducted on porphyrin-based hybrid materials containing gold nanoparticles or polyvinylpyrrolidone bring further original contributions and demonstrate that porphyrins preserve their aggregation ability even in metallic and polymeric hybrid materials despite their very low concentration level (ppm).
- Electrochemical analysis of porphyrins using cyclic voltammetry clearly showed the versatility of the porphyrin macrocycle, capable of undergoing both oxidation and reduction processes, irrespective of substituents nature, the presence of a central metal ion, the type of the working electrode and the solvent - supporting electrolyte system.
- The free base porphyrin derivatives were oxidized in two stages at the porphyrin macrocycle resulting in the formation of π-cation radicals and dications. Mono- and diprotonated intermediate species generated during the electrochemical experiments were identified using UV-Vis spectroscopy.
- Studies performed on novel porphyrin structures aiming to identify their practical applications resulted in the formulation and testing of several efficient potentiometric sensors using porphyrin ionophores that are capable of detecting heavy metals and anions of medical and environmental importance.
- The porphyrin-based sensor using 5-(4-pyridyl)-10,15,20-tris(phenoxyphenyl)porphyrin as ionophore showed sensibility and selectivity toward Cr^{3+} ions, a slope of 18.11 mV/decade over the $3 \times 10^{-5} \div 10^{-1}$ M concentration range and a detection limit of 9×10^{-6} M.
- A perchlorate-selective sensor was manufactured using Co(II) 5,10,15,20-tetrakis (3-hydroxyphenyl)porphyrin as ionophore and showed remarkable properties that placed it next to the best potentiometric sensors of this type reported in the literature. The sensor exhibited a near-Nernstian slope of 58.95 mV/decade in the $5 \times 10^{-7} \div 10^{-1}$ M concentration range. The sensor showed a detection limit of 3×10^{-7} M and was stable in the pH range 2.5 ÷ 12.
- The importance of plasticizer selection on the detection properties of sensors using Zn(II) 5,10,15,20-tetrakis(3,4-dimethoxyphenyl)porphyrin as ionophore was demonstrated by formulating and testing perchlorate-, thiocyanate- and iodide-selective sensors.

- The corrosion inhibition ability of 5,10,15,20-tetrakis(4-pyridyl)porphyrin was studied and demonstrated for carbon steel samples in aggressive acidic media (H_2SO_4 5%). The corrosion inhibition efficiency of the porphyrin was over 50% and its presence in the acidic solution decreased the corrosion rate by covering the metal surface with multilayer structures.

References

1. Lensen M.C., Takazawa K., Elemans J.A.A.W., Jeukens C.R.L.P.N., Christianen P.C.M., Maan J.C., Rowan A.E., Nolte R.J.M., Aided self-assembly of porphyrin nanoaggregates into ring-shaped architectures, *Chem. Eur. J.*, **2004**, 10, 831-839;

2. Fagadar-Cosma E., Fagadar-Cosma G., Vasile M., Enache C., Synthesis, spectroscopic and self-assembling characterization of novel photoactive mixed aryl-substituted porphyrin, *Curr. Org. Chem.*, **2012**, 16, 931-941;

3. Byrn M.P., Curtis C.J., Hsiou Y., Khan S.I., Sawin P.A., Tendick S.K., Terzis A., Strouse C.E., Porphyrin sponges: conservative of host structure in over 200 porphyrin-based lattice clathrates, *J. Am. Chem. Soc.*, **1993**, 115, 9480-9497;

4. Fagadar-Cosma E., Sebarchievici I., Lascu A., Creanga I., Palade A., Birdeanu M., **Taranu B.**, Fagadar-Cosma G., Optical and electrochemical behavior of new nano-sized complexes based on gold-colloid and Co-porphyrin derivative in the presence of H_2O_2, *J. Alloy. Compd.*, **2016**, 686, 896-904;

5. Fagadar-Cosma E., Tarabukina E., Zakharova N., Birdeanu M., **Taranu B.**, Palade A., Creanga I., Lascu A., Fagadar-Cosma G., Hybrids formed between polyvinylpyrrolidone and an A_3B porphyrin dye: behaviour in aqueous solutions and chemical response to CO_2 presence, *Polymer Int.*, **2016**, 65, 200-209;

6. Tutunea F., Ryan M.D., Visible and infrared spectroelectrochemistry of cobalt porphinones and porphinediones, *J. Electroanal. Chem.*, **2012**, 670, 16-22;

7. Fagadar-Cosma E., Vlascici D., Fagadar-Cosma G., Bizerea O., Chiriac A., Studiu asupra comportamentului electrochimic al metaloporfirinelor cu Co(II) şi Co(III). Electrod nitrit-selectiv pe bază de clorură de [5,10,15,20-tetrafenil-21H,23H-porfirinat-N21,N22,N23,N24] cobalt(III), *Rev. Chim. (Bucharest)*, **2004**, 55, 882-885;

8. **Taranu B.O.**, Vlascici D., Sebarchievici I., Fagadar-Cosma E., The aggregation behavior of an A_3B free base porphyrin and its application as chromium(III)-selective membrane sensor, *Stud. U. Babes-Bol. Che.*, **2016**, LXI, 199-212;

9. Fagadar-Cosma G., **Taranu B.O.**, Birdeanu M., Popescu M., Fagadar-Cosma E., Influence of 5,10,15,20-tetrakis(4-pyridyl)-21H,23H-porphyrin on the corrosion of steel in aqueous sulfuric acid, *Dig. J. Nanomater. Bios.*, **2014**, 9, 551-557.